Molecular Vision 2024; 30:160-166 <http://www.molvis.org/molvis/v30/160>
Received 22 October 2023 | Accepted 20 March 2024 | Published 22 March 2024

Uveal melanoma cell lines Mel270 and 92.1 exhibit a mesenchymal phenotype and sensitivity to the cytostatic effects of transforming growth factor beta in vitro

Coralie Doudnikoff,[1] Delphine Leclerc,[2] Gaëlle Angenard,[3] David Gilot,[2] Cédric Coulouarn,[2] Frederic Mouriaux[1,2]

(The first two authors contributed equally to this work and are considered as first authors.)

(The last two authors contributed equally and considered as senior authors.)

[1]Service d'Ophtalmologie, CHU Rennes, Rennes, France; [2]INSERM U1242, OSS, Université Rennes, Rennes, France; [3]INSERM U1317, NuMeCan, INRAE, Université de Rennes, Rennes, France

Purpose: Uveal melanoma (UM) is a deadly cancer with limited therapeutic options. At advanced stages, UM cells metastasize almost exclusively into the liver, where targeting metastatic UM cells remain a clinical challenge. Transforming growth factor beta (TGF-β) exhibits a functional duality in cancer, with one arm limiting tumor growth at an early stage and the second arm promoting metastasis at an advanced stage, notably by inducing an epithelial-to-mesenchymal transition. Thus, we hypothesized that targeting the TGF-β pathway could be relevant in the treatment of metastatic UM.
Methods: In this study, we first characterized the pseudoepithelial/mesenchymal phenotype of UM cell lines Mel270 and 92.1. We then treated the cell lines with TGF-β to evaluate their responsiveness to the cytokine and to characterize the functional impact of TGF-β on their cell viability.
Results: The results demonstrated, first, that the UM cell lines exhibited a mesenchymal phenotype and responded to TGF-β treatment in vitro and, second, that TGF-β promoted a cytostatic effect on the UM cell lines.
Conclusions: Our findings indicate that UM cells are sensitive to the two arms of TGF-β signaling, which suggests that targeting the TGF-β pathway could be challenging in UM and would require a precise selection of patients in which only the prometastatic arm of TGF-β is activated.

Uveal melanoma (UM) is the most common primary intraocular tumor in adults and represents approximately 5% of all melanomas [1]. This aggressive cancer affects approximately 1 to 9 persons per million population per year [2]. This tumor localizes preferentially in the choroid [2,3]. However, despite effective treatment of the primary tumor, patients may still develop metastases within a few years, almost exclusively in the liver [2]. Currently, the approved treatments for metastatic UM are limited; thus, UM often lead to fatality within 1 to 2 years. While tebentafusp is effective, its application is restricted to HLA-A*02:01-positive patients [4], and selective hepatic perfusion treatment is constrained to cases with isolated liver metastases. The challenges in developing new therapeutic susceptibilities include better understanding of the reason why UM metastasizes preferentially to the liver and identification of the key drivers of this process.

Correspondence to: Frederic Mouriaux, INSERM U1242 OSS, Service d'Ophtalmologie, CHU Rennes, 2 Rue Henri le Guilloux, 35000 Rennes, France; email: frederic.mouriaux@chu-rennes.fr

Cytokines are soluble proteins that act through cell-cell communication. By remodeling the tumor microenvironment, cytokines support cancer cell growth, differentiation, migration, and metastasis [5]. Transforming growth factor beta (TGF-β) is a pleiotropic cytokine that exerts a wide range of functions from embryogenesis to tissue homeostasis in adults. In addition, TGF-β contributes to several hallmarks of cancer [6,7]. TGF-β activity is highly dependent on the cellular context and tissue microenvironment. Thus, at the early stages of carcinogenesis, TGF-β exerts cytostatic functions, while in later stages, its activity shifts to tumor-promoting functions, including metastasis, as a potent inducer of epithelial-to-mesenchymal transition (EMT) [8]. Previous works of our team demonstrated that specific *TGF-β* gene expression signatures can predict patient prognosis in hepatocellular carcinoma (HCC) [9] and induce the expression of EMT-associated transcription factor FOXS1 [10]. Several inhibitors are currently under clinical evaluation in several cancers, including HCC (NCT01246986) [11,12]. Moreover, previous works have demonstrated that TGF-β

controls metastasis development, notably in breast cancer and cutaneous melanoma [13,14]. Thus, inhibition of the TGF-β pathway in choroidal melanoma may represent a promising therapeutic approach.

In this study, we hypothesized that as UM metastasizes, especially in the liver, where the microenvironment facilitates TGF-β signaling, the TGF-β pathway might be activated in the UM cells. Thus, the aim of this study was to characterize the TGF-β activity in UM cells.

METHODS

Cell culture conditions: Mel270 [15] and 92.1 [16] cell lines originate from primary uveal melanoma (UM) tumors diagnosed in patients who have developed metastases [17]. The Mel270 cell line was kindly provided by Dr. Martine Jager (University of Leiden, The Netherlands), and the 92.1 cell line was obtained from the European Collection of Authenticated Cell Cultures. Cell line authentication was confirmed using short tandem repeat analysis. UM cells were cultivated in a humidified atmosphere (37 °C, 5% CO_2) with RPMI 1640 medium supplemented with 10% (Mel270) or 20% (92.1) fetal bovine serum (FBS; HyClone, Logan, UT), 1% L-glutamine (except 92.1), and 1% penicillin-streptomycin. The cells were regularly tested for mycoplasma using a MycoAlert Mycoplasma Detection Kit (Lonza, Bâle, Switzerland).

Immunofluorescence: The cells were seeded in 96-well plates. When the cells reached confluency, they were fixed with 4% paraformaldehyde for 15 min, washed 3 times in phosphate-buffered saline (PBS), and blocked for 1 h in PBS/5% FBS/0.3% Triton X-100. The primary antibodies used for immunofluorescent staining were rabbit anti-vimentin (1:200; No. 5741S, Cell Signaling Technology, Danvers, MA) and rabbit anti-E-cadherin (1:100, No. 3195, Cell Signaling Technology). After overnight incubation with primary antibodies, the cells were washed 3 times with PBS and then incubated with the secondary antibody Dylight 488 goat anti-rabbit (1:400; Eurobio Scientific, Les Ulis, France) for 1 h in the presence of Hoechst 333,442 (1:5000; ThermoScientific, Waltham, MA). The cells were observed under a fluorescence microscope at 470 nm for the secondary antibody and 365 nm for Hoechst. Acquired images were analyzed with the ImageJ software.

TGF-β and galunisertib treatments: UM cells were seeded in 6-well plates. When the cells reached approximately 70% confluency, FBS starvation was performed for 8 h. Four different treatments were then performed in a FBS-free medium as follows: 1) control (solvent alone), 2) TGF-β (1 ng/ml TGF-β1; R&D Systems, Minneapolis, MN), 3) galunisertib (10 mM; Interchim, Montluçon, France), and 4) TGF-β + galunisertib (1 ng/ml TGF-β1 + 10 mM galunisertib). TGF-β1 was diluted in 0.1% bovine serum albumin (BSA), 4 mM HCl, and galunisertib with dimethyl sulfoxide (DMSO). Unless otherwise indicated, the treatments were performed for 16 h.

Cell viability assay: Mel270 and 92.1 were seeded in triplicate in 96-well plates at a density of 5.0×10^3 and 1.0×10^4 cells/well, respectively. Cell lines were treated with TGF-β (1 ng/ml TGF-β), galunisertib (10 mM LY2157299), or combined treatments for 16 h, 8 h after cell seeding. When cells were incubated for more than 2 days in culture, the same treatment was re-applied on day 2. Cell viability was assessed using a colorimetric assay on the basis of the enzymatic reduction of a yellow tetrazolium salt substrate [3-(4,5-dimethylthiazol-2-yl)-2,5-diphenyltetrazolium bromide, MTT; Sigma M2128–250MG] into purple insoluble formazan by metabolically active cells, in accordance with the manufacturer's instructions. Briefly, after removing the cell medium, the cells were incubated with 100-µL MTT substrate for 4 h at 37 °C. Subsequently, the solution was aspirated, and the resulting formazan product was dissolved with 100 µl of DMSO. After 5 min of shaking, absorbance was measured at 535 nm (Polar Star, BMG Labtec).

Protein extraction and western blotting analysis: The cells were lysed chemically using a radioimmunoprecipitation assay lysis buffer (ThermoScientific) supplemented with phosphatase and protease inhibitors (Roche, Bâle, Switzerland). A western blot analysis was performed as previously described [10]. Membranes were initially incubated for 2 h in a blocking solution (TBS-Tween-0.1% + 5% BSA) followed by overnight incubation at 4 °C with a primary antibody: β-Actin (1:1000; No. 8457; Cell Signaling Technology), E-cadherin (1:1000; No. 3195, Cell Signaling Technology), vimentin (1:1000; No. 5741S, Cell signaling Technology), P-SMAD3 (1:1000; No. 9520T, Cell Signaling Technology), P-SMAD2 (1:1000; No. 3108P, Cell Signaling Technology), SMAD3 (1:100; No. 9523P, Cell Signaling Technology), or SMAD2 (1:100; No. 5339P, Cell Signaling Technology). After three washes with TBS-Tween-0.1%, the membrane was incubated for 1 h with an HRP-linked secondary antibody (anti-rabbit IgG, 1:1000; No. 7074, Cell Signaling Technology), and the membrane was incubated for 1 h. Detection was performed using a chemiluminescent substrate reagent (Western ECL Select, GE Healthcare, Chicago, IL).

RNA extraction and quantitative reverse-transcription polymerase chain reaction: RNA was directly extracted from the cell culture plates using a miRNAeasy kit (Qiagen, Hilden, Germany) and quantified using a nanodrop. Quantitative reverse-transcription polymerase chain reaction (RT-PCR)

was performed as previously described [10], starting from 1-µg total RNA. Briefly, reverse transcription was performed using a Superscript III RT enzyme (Invitrogen), and quantitative PCR was performed using the SYBR Green Master Mix (Applied Biosystems). The primers used (Eurogentec) are listed in Appendix 1, and the TATA-binding protein was used as the internal control for normalization. The results were analyzed using the StepOne v2.3 software. Relative expressions were compared with the control group using the $2^{-\Delta\Delta Ct}$ method.

RESULTS

Mel270 and 92.1 UM cell lines exhibited a mesenchymal phenotype: We first characterized the pseudoepithelial/mesenchymal phenotype of UM cell lines to evaluate their degree of tumor progression. The presence of Mel270 and 92.1 expressions were established in primary UMs from patients who developed metastases [17]. Immunofluorescent staining demonstrated that Mel270 and 92.1 cells do not express E-cadherin ($CDH1^-$) but express vimentin (VIM^+; Figure 1A). These results were confirmed by the results of western blot experiments that showed the presence of VIM expression but the absence of CDH1 expression (Figure 1B) in both cell lines. Thus, Mel270 and 92.1 already lost their pseudoepithelial identity and switched to a mesenchymal state, consistent with the results of previous studies that associated UM cell line aggressivity [18] and UM metastatic phenotype with high vimentin and low E-cadherin expression levels [19,20].

Mel270 and 92.1 UM cell lines exhibited sensitivity to TGF-β treatment: We next performed TGF-β treatments to evaluate if the TGF-β pathway is active in these cell lines in vitro. First, we conducted a time course experiment to analyze the TGF-β activation. Our results demonstrated that Mel270 responded to TGF-β and that the highest activation rate was obtained after 2 h of treatment, as exemplified by SMAD2/3 phosphorylation (Figure 2A). We next tested the specificity of the response by performing a galunisertib treatment (LY2157299, an inhibitor of the type 1 TGF-β receptor, TGFBR1). Our results indicated that SMAD2/3 phosphorylation was dependent on TGF-β activation through TGFBR1, as expected (Figure 2B–D). The results obtained from the 92.1 cells showed that P-SMAD2 and P-SMAD3 appeared to be poorly regulated by TGF-β compared with the Mel270 cells (Figure 2B). However, the pathway was still activated, as the canonical TGF-β target genes (SMAD-dependent) were induced in both cell lines. Our experiment results showed that the expression of *SERPINE1*, a serine protease inhibitor transcriptionally activated by SMAD2/SMAD3, was induced more than tenfold after TGF-β treatment. The expression of *SMAD7*, a TGF-β antagonist acting through negative feedback, was also clearly induced in the 92.1 cells (Figure 2E), supporting the activation of the SMAD-dependent TGF-β pathway. Even if the *SMAD7* expression in Mel270 cells was unclear (Figure 2E), differences in the origins and genetic backgrounds of the cell lines likely explain these phenotypic variations. We then performed a functional analysis (viability assay) to evaluate whether the cell lines might be sensitive to the cytostatic effect of TGF-β. Surprisingly, we observed a slight decrease in the cell density after 3 or 4 days of treatment (Figure 2F).

Taken together, our results demonstrate that although the 92.1 and Mel270 cell lines exhibited a mesenchymal phenotype, they not only responded to the TGF-β treatment but also were sensitive to its cytostatic effects in vitro.

DISCUSSION

In this study, we evaluated the impact of TGF-β, a pleiotropic cytokine involved in numerous cancers, including liver tumors [9,10], in primary UM cell lines in vitro (92.1 and Mel270). In summary, our results show that Mel270 and 92.1 expressed a mesenchymal phenotype, consistent with their ability to invade and develop metastases. Functional analyses demonstrated that the TGF-β pathway can be activated in these cell lines through the SMAD-dependent canonical pathway, and this activation leads to a slight reduction in cell viability in vitro. While further experiments are needed to confirm these findings in other UM cell lines, replicating the complexity of liver metastasis regulation in vitro is challenging because of multiple influencing factors. While we observed a weak antitumorigenic effect on cell density, whether TGF-β reduces proliferation or induces cell death in these cells and whether this observation is true at different UM progression steps remain to be clarified. Questions regarding adhesion, invasion, and migration properties might be interesting to investigate. One other interesting point is whether TGF-β can induce EMT in UM, as already demonstrated in HCC by our team [10].

Other research groups have studied the functional effect of TGF-β on UM cells. For instance, a previous study demonstrated that TGF-β inhibits the invasion of UM cell lines in vitro [21], thus confirming its antitumoral role, as we also observed in the present study. It was also reported that paradoxically, TGF-β1 secretion by UM cells promotes liver metastatic colonization through crosstalk with hepatic stellate cells and extracellular matrix remodeling, highlighting a protumoral effect of TGF-β1 [22]. These observations were also validated in vivo. In a mouse model of intra-splenically

inoculated Mel270-luc cells, mice treated with SB525334 (an inhibitor of TGFBR1) presented less bioluminescence signal and metastatic nodules in the liver than mice treated with the vehicle [22]. These conflicting results raise the question of whether the TGF-β ligands from the liver microenvironment act directly on cancer cells and/or indirectly through stromal cells and illustrate the complexity of studying metastasis. Thus, TGF-β may exert tumor-suppressive or tumor-promoting functions depending on the tumor stage of UM, highlighting its functional duality, as observed in other types

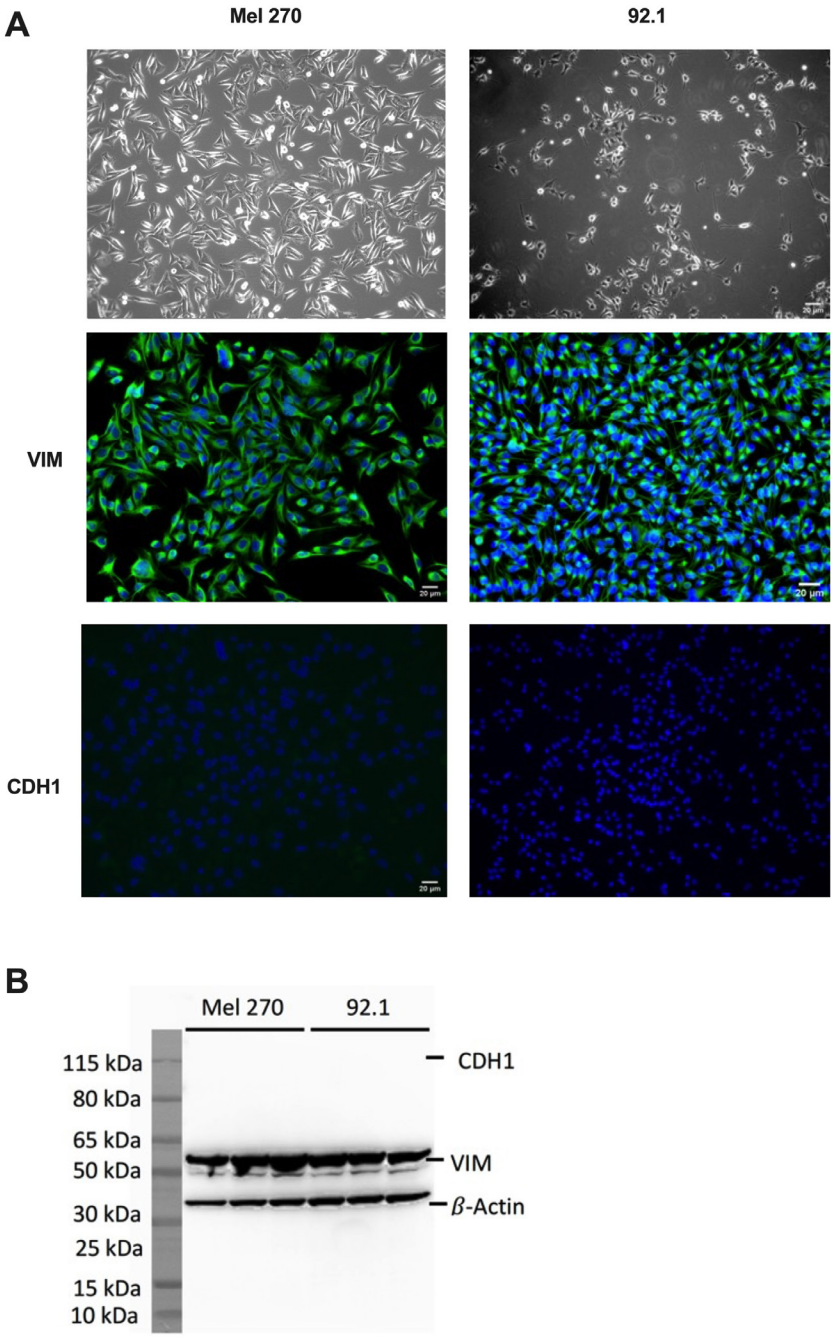

Figure 1. Phenotypic characterization of UM cell lines. **A**: Representative immunofluorescence images of Mel 270 and 92.1 cell lines stained with anti-vimentin (VIM) and anti-E-cadherin (CDH1) proteins (with the color green indicating a positive signal), colabeled with Hoechst (blue) to visualize the nuclei. Scale bar = 20 µm. **B**: Western blot analysis of VIM and CDH1 expressions in Mel270 and 92.1 cell lines, using β-actin as a loading control (n = 3 biological replicates, one in each lane).

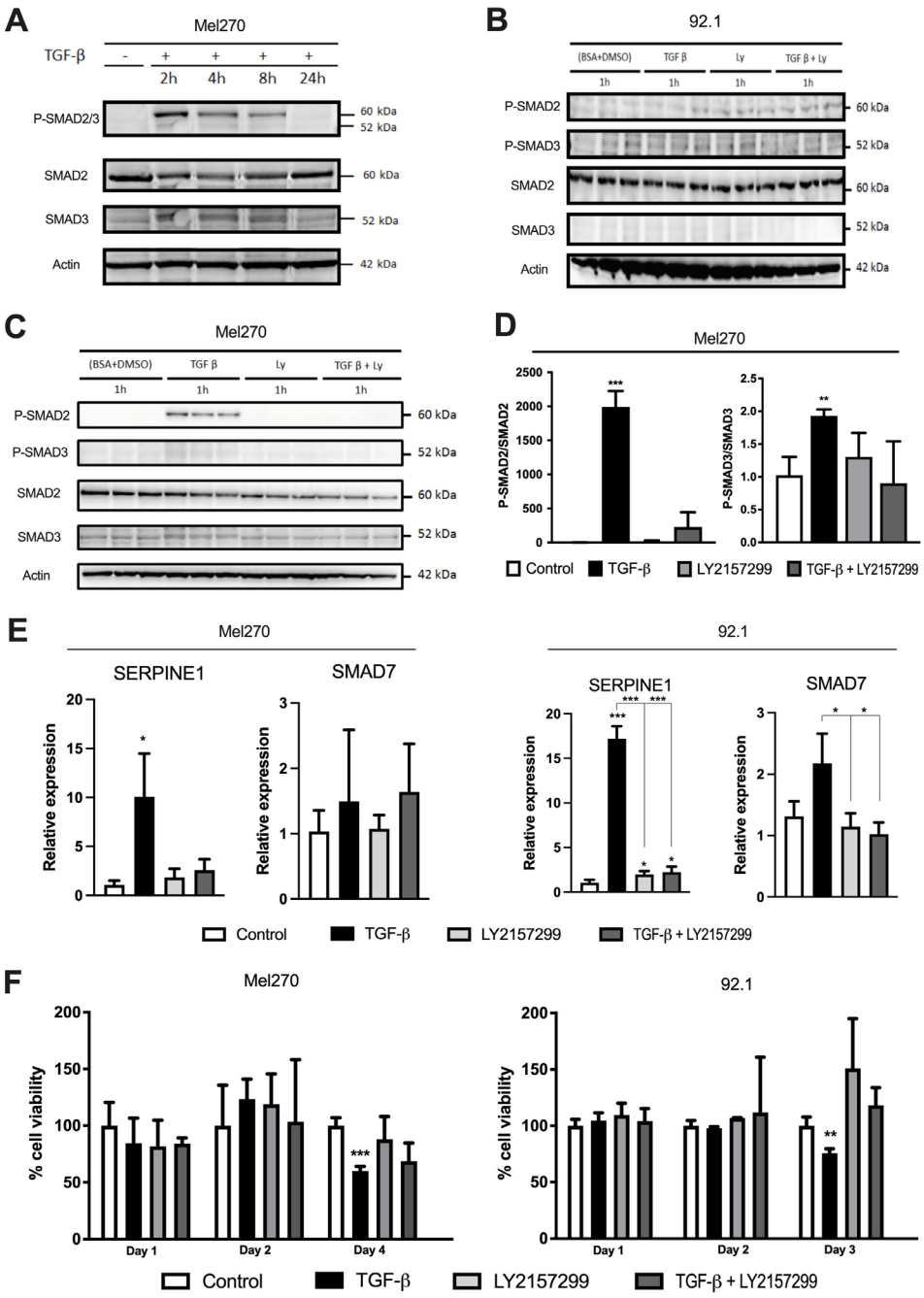

Figure 2. TGF-β pathway activation in UM cell lines. **A**: Western blot analysis of SMAD2, SMAD3, and phospho-SMAD2/3 expressions in response to TGF-β treatment (1 ng/ml TGF-β, time course experiment from 2 to 24 h of treatment) in the Mel270 cell line, using β-actin as a loading control in all western blot experiments (n = 1 biological replicate). **B** and **C**: Western blot analysis of SMAD2, SMAD3, and phospho-SMAD2/3 expressions in response to TGF-β, Ly (LY2157299, type 1 TGF-β receptor inhibitor), or a combined treatment (1 ng/mL TGF-β and 10 mM LY2157299; 1 h; n = 3 biological replicates). **D**: Quantification of phospho-SMAD2/SMAD2 and phospho-SMAD3/SMAD3 Mel270 western blot signal intensities relative to **(C)** (n = 3 biological replicates). **E**: Expression levels of 2 well-known TGF-β target genes (*SERPINE1* and *SMAD7*) in UM cell lines in response to TGF-β, LY2157299 (type 1 TGF-β receptor inhibitor) or a combined treatment (1 ng/ml TGF-β and 10 mM LY2157299; 16 h), evaluated using RT-qPCR (n = 3 biological replicates). **F**: Cell viability evaluated using a MTT [3-(4,5-dimethylthiazol-2-yl)-2,5-diphenyltetrazolium bromide] assay in UM cell lines in response to TGF-β, LY2157299, or a combined treatment (1 ng/ml TGF-β and 10 mM LY2157299; 16 h) from days 1 to 4 after treatment. When cells were incubated for more than 2 days in culture, the same treatment was reapplied on day 2 (n = 3 biological replicates). Statistical analyses for (**D–F**) were performed using a *t* test. Data are presented as mean ± SD from three independent biological replicates. *p < 0.05, **p < 0.01, ***p < 0.001. TGFβ, transforming growth factor β; Ly, LY2157299; P-SMAD2, phospho-SMAD2; P-SMAD3, phospho-SMAD3; BSA, BSA, DMSO, dimethylsulfoxyde.

of cancer [8]. In conclusion, targeting the TGF-β pathway in metastatic UM should take into account the sensitivity of tumor cells to the cytostatic effects of TGF-β. In this context, specific biomarkers should also be developed in the future to identify patients with UM who may benefit from inhibition of the TGF-β pathway.

APPENDIX 1. SUPPLEMENTARY TABLE 1.

To access the data, click or select the words "Appendix 1." List of primers.

ACKNOWLEDGMENTS

Authorship contribution: Coralie Doudnikoff: Conceptualization, Data curation, Formal analysis, Investigation, Visualization, Validation, Writing – review & editing Delphine Leclerc: Visualization, Validation, Writing – original draft, Writing – review & editing Gaëlle Angenard: Data curation, Investigation – review & editing David Gilot: Resources, Investigation, Writing – review & editing Cédric Coulouarn: Conceptualization, Data curation, Formal analysis, Investigation, Visualization, Validation, Writing – original draft, Writing – review & editing, Project administration. Frederic Mouriaux: Conceptualization, Data curation, Formal analysis, Investigation, Visualization, Validation, Writing – original draft, Writing – review & editing, Project administration. **Funding information:** Authors would like to thanks their sponsors: CD is funded by funded by Fonds de recherche en opthtalmologie (CHU Rennes). DL is funded by Ministère de l'enseignement Supérieur, de la Recherche et de l'Innovation (PhD fellowship). CC is funded by Inserm, University of Rennes 1, Ligue Contre le Cancer (CD22, CD35, CD44, CD85), Fondation ARC, French Ministry of Health and the French National Cancer Institute (PRT-K20–136, CHU Rennes, CLCC Eugène Marquis, Rennes). DG is funded by Aviesan Plan Cancer and Canceropôle Grand-Ouest.

REFERENCES

1. Singh AD, Turell ME, Topham AK. Uveal melanoma: trends in incidence, treatment, and survival. Ophthalmology 2011; 118:1881-5. [PMID: 21704381].

2. Jager MJ, Shields CL, Cebulla CM, Abdel-Rahman MH, Grossniklaus HE, Stern MH, Carvajal RD, Belfort RN, Jia R, Shields JA, Damato BE. Uveal melanoma. Nat Rev Dis Primers 2020; 6:24-[PMID: 32273508].

3. Shields CL, Kaliki S, Shah SU, Luo W, Furuta M, Shields JA. Iris melanoma: features and prognosis in 317 children and adults. J AAPOS 2012; 16:10-6. [PMID: 22370659].

4. Hassel JC, Piperno-Neumann S, Rutkowski P, Baurain JF, Schlaak M, Butler MO, Sullivan RJ, Dummer R, Kirkwood JM, Orloff M, Sacco JJ, Ochsenreither S, Joshua AM, Gastaud L, Curti B, Piulats JM, Salama AKS, Shoushtari AN, Demidov L, Milhem M, Chmielowski B, Kim KB, Carvajal RD, Hamid O, Collins L, Ranade K, Holland C, Pfeiffer C, Nathan P. Three-Year Overall Survival with Tebentafusp in Metastatic Uveal Melanoma. N Engl J Med 2023; 389:2256-66. [PMID: 37870955].

5. Propper DJ, Balkwill FR. Harnessing cytokines and chemokines for cancer therapy. Nat Rev Clin Oncol 2022; 19:237-53. [PMID: 34997230].

6. Derynck R, Turley SJ, Akhurst RJ. TGFβ biology in cancer progression and immunotherapy. Nat Rev Clin Oncol 2021; 18:9-34. [PMID: 32710082].

7. Tian M, Neil JR, Schiemann WP. Transforming growth factor-β and the hallmarks of cancer. Cell Signal 2011; 23:951-62. [PMID: 20940046].

8. Ikushima H, Miyazono K. TGFbeta signalling: a complex web in cancer progression. Nat Rev Cancer 2010; 10:415-24. [PMID: 20495575].

9. Coulouarn C, Factor VM, Thorgeirsson SS. Transforming growth factor-beta gene expression signature in mouse hepatocytes predicts clinical outcome in human cancer. Hepatology 2008; 47:2059-67. [PMID: 18506891].

10. Bévant K, Desoteux M, Angenard G, Pineau R, Caruso S, Louis C, Papoutsoglou P, Sulpice L, Gilot D, Zucman-Rossi J, Coulouarn C. TGFβ-induced FOXS1 controls epithelial-mesenchymal transition and predicts a poor prognosis in liver cancer. Hepatol Commun 2022; 6:1157-71. [PMID: 34825776].

11. Ciardiello D, Elez E, Tabernero J, Seoane J. Clinical development of therapies targeting TGFβ: current knowledge and future perspectives. Ann Oncol 2020; 31:1336-49. [PMID: 32710930].

12. Faivre S, Santoro A, Kelley RK, Gane E, Costentin CE, Gueorguieva I, Smith C, Cleverly A, Lahn MM, Raymond E, Benhadji KA, Giannelli G. Novel transforming growth factor beta receptor I kinase inhibitor galunisertib (LY2157299) in advanced hepatocellular carcinoma. Liver Int 2019; 39:1468-77. [PMID: 30963691].

13. Kang Y, He W, Tulley S, Gupta GP, Serganova I, Chen C-R, Manova-Todorova K, Blasberg R, Gerald WL, Massagué J. Breast cancer bone metastasis mediated by the Smad tumor suppressor pathway. Proc Natl Acad Sci U S A 2005; 102:13909-14. [PMID: 16172383].

14. Javelaud D, Mohammad KS, McKenna CR, Fournier P, Luciani F, Niewolna M, André J, Delmas V, Larue L, Guise TA, Mauviel A. Stable overexpression of Smad7 in human melanoma cells impairs bone metastasis. Cancer Res 2007; 67:2317-24. [PMID: 17332363].

15. Chen PW, Murray TG, Uno T, Salgaller ML, Reddy R, Ksander BR. Expression of MAGE genes in ocular melanoma during progression from primary to metastatic disease. Clin Exp Metastasis 1997; 15:509-18. [PMID: 9247253].

16. De Waard-Siebinga I, Blom DJ, Griffioen M, Schrier PI, Hoogendoorn E, Beverstock G, Danen EH, Jager MJ. Establishment and characterization of an uveal-melanoma cell line. Int J Cancer 1995; 62:155-61. [PMID: 7622289].

17. Jager MJ, Magner JAB, Ksander BR, Dubovy SR. (2016) Uveal Melanoma Cell Lines: Where do they come from? (An American Ophthalmological Society Thesis). Trans Am Ophthalmol Soc 114:T5.

18. Duan F, Lin M, Li C, Ding X, Qian G, Zhang H, Ge S, Fan X, Li J. Effects of inhibition of hedgehog signaling on cell growth and migration of uveal melanoma cells. Cancer Biol Ther 2014; 15:544-59. [PMID: 24553082].

19. Venza M, Visalli M, Catalano T, Biondo C, Beninati C, Teti D, Venza I. DNA methylation-induced E-cadherin silencing is correlated with the clinicopathological features of melanoma. Oncol Rep 2016; 35:2451-60. [PMID: 26883095].

20. Linge A, Kennedy S, O'Flynn D, Beatty S, Moriarty P, Henry M, Clynes M, Larkin A, Meleady P. Differential expression of fourteen proteins between uveal melanoma from patients who subsequently developed distant metastases versus those who did Not. Invest Ophthalmol Vis Sci 2012; 53:4634-43. [PMID: 22570344].

21. Woodward JKL, Elshaw SR, Murray AK, Nichols CE, Cross N, Laws D, Rennie IG, Sisley K. Stimulation and inhibition of uveal melanoma invasion by HGF, GRO, IL-1alpha and TGF-beta. Invest Ophthalmol Vis Sci 2002; 43:3144-52. [PMID: 12356817].

22. Dai W, Liu S, Wang S, Zhao L, Yang X, Zhou J, Wang Y, Zhang J, Zhang P, Ding K, Li Y, Pan J. Activation of transmembrane receptor tyrosine kinase DDR1-STAT3 cascade by extracellular matrix remodeling promotes liver metastatic colonization in uveal melanoma. Signal Transduct Target Ther 2021; 6:176-[PMID: 33976105].

Articles are provided courtesy of Emory University and the Zhongshan Ophthalmic Center, Sun Yat-sen University, P.R. China. The print version of this article was created on 22 March 2024. This reflects all typographical corrections and errata to the article through that date. Details of any changes may be found in the online version of the article.